

## News & Views

### Is the Distribution of Tissue $pO_2$ Homogeneous?

AMY G. TSAI,<sup>1,2</sup> PAUL C. JOHNSON,<sup>1</sup> and MARCOS INTAGLIETTA<sup>1,2</sup>

#### ABSTRACT

Oxygen transport from blood to the mitochondria is dependent on oxygen gradients. The interstitial or extracellular  $pO_2$ , measured by the phosphorescence-decay method, is indicative of these driving forces and the amount of oxygen available to the mitochondria. Diverse protocols for sampling tissue  $pO_2$  show that measurements sampling only interstitial  $pO_2$  levels provide a reliable measurement of the tissue  $pO_2$  level. Present findings lead to the hypothesis that tissue has a fairly uniform interstitial fluid  $pO_2$  level and that local inhomogeneity due to the presence arteriolar and venular vessels is smoothed out by the steep gradients at the microvascular walls. *Antioxid. Redox Signal.* 9, 979–984.

#### MICROVASCULAR $pO_2$ DISTRIBUTION

THE RATIONALE for the level of interstitial  $pO_2$  found in tissues is not well understood. This level should reflect the existence of both an appropriate gradient between the extracellular environment and mitochondria, and a safety margin that prevents  $pO_2$  falling below the level needed to maintain the gradient. The moment-to-moment changes in oxygen supply and the presence of different anatomic features also suggest a variability of tissue  $pO_2$ . Blood microvessels conveying arterial blood should in principle have relatively high perivascular  $pO_2$ . In contrast, venules should have a significantly lower perivascular  $pO_2$ , as they have a significantly lower intravascular  $pO_2$  because of the release of oxygen from the blood during its transit from the arterioles because of the oxygen sink created by the tissue's metabolic rate. These features suggest the presence of an intravascular and extravascular "longitudinal oxygen gradient" running from the arterial input to the venular exit.

The potential extravascular  $pO_2$  heterogeneity has not been supported by measurements obtained from *in vivo* studies (20).  $pO_2$  measurements made with different techniques and in different tissues confirm the presence of the intravascular longitudinal  $pO_2$  gradient from arterioles to capillaries (6, 13). However, this gradient reverses in the venules as diffusion, an-

atomic pairing with countercurrent flows, and convective shunts transport some of the oxygen from the arterioles to the venules (7, 8). Comparatively large oxygen gradients at the arteriolar and venular walls have been found and may be a mechanism whereby the higher blood  $pO_2$  is reduced to a perivascular  $pO_2$  level in close proximity of the overall average interstitial  $pO_2$ . The wall gradient, in combination with the U-shaped intravascular longitudinal oxygen gradient, causes  $pO_2$  to be fairly uniformly distributed throughout the tissue and relatively unaffected by the proximity of arterioles and venules. This configuration of tissue  $pO_2$  is implicit in the results obtained from studies in the hamster window-chamber preparation (10, 13) but is not specifically demonstrated with these systematic surveys of microvascular  $pO_2$  distribution. The relatively uniform interstitial  $pO_2$  level characteristic has been challenged by new techniques for mapping the distribution of intra- and extravascular  $pO_2$ . A recently developed technique based also on phosphorescence quenching to measure  $pO_2$  found that nearly 60% of skeletal muscle at rest had  $pO_2$  levels >50 mm Hg (23). Previously investigators have reported that average tissue  $pO_2$  was closely regulated to ~20–23 mm Hg (20). Discrepancies between tissue  $pO_2$  levels found in the literature reflect in part the difficulty in assessing this parameter and its dependence on the measurement technique.

<sup>1</sup>Department of Bioengineering, University of California, San Diego, La Jolla, California.

<sup>2</sup>La Jolla Bioengineering Institute, La Jolla, California.

### Using Pd-phosphorescence-quenching microscopy to measure interstitial and tissue $pO_2$

Oxygen-tension measurements are made by using the Pd-phosphorescence-quenching method (PQM) developed by Wilson *et al.* (21) implemented for microcirculatory studies (12). This noninvasive method is based on the oxygen-dependent quenching of phosphorescence emitted by albumin-bound metalloporphyrin complex after pulsed light excitation, where the decay rate of the light-excited phosphorescence is inversely proportional to the partial pressure of oxygen, according to the Stern-Volmer equation. PQM has been used in this preparation for both intravascular and extravascular oxygen-tension measurements, as albumin exchange between plasma and tissue allows sufficient concentrations of albumin-bound dye within the interstitium to achieve an adequate signal-to-noise ratio (3, 19). Animals receive a slow intravenous injection of 15 mg/kg body weight at a concentration of 10.1 mg/ml of a palladium-meso-tetra (4-carboxyphenyl) porphyrin (Porphyrin Products, Inc., Logan, UT). The dye is allowed to circulate for 10 min before oxygen measurements.

In our system, intravascular measurements are made by placing an adjustable optical rectangular (or square) window on the blood vessel or tissue location of interest. The size of the window is adjusted depending on the resolution required for the measurement, which can be made within the microvessel, in its immediate vicinity, or in the tissue void of microvessels.

### Random vs. focused tissue $pO_2$ measurements

Tissue  $pO_2$  measurements were performed according to two procedures: **Random protocol:**  $pO_2$  measurements were made along five vertical pathways and three horizontal pathways (Fig. 1). The microscope field was advanced in  $\sim 150$ - $\mu m$  steps along each pathway, and  $pO_2$  was measured. This

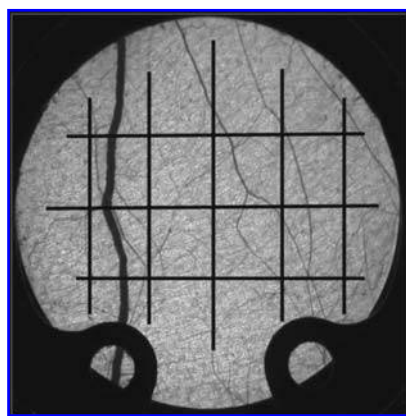


**FIG. 1. Hamster window chamber with superimposed paths used for the random protocol.** The window has a diameter of 12  $\mu m$ . In each animal, the pathlines are drawn and measurement made by following the random protocol on the superimposed paths in 100- $\mu m$  increments. After each pathway is completed, two to three focused measurements are performed in the adjacent area.

method is random, in the sense the target may include any combination of intravascular, perivascular, or interstitial tissue. **Focused protocol:** Interstitial tissue  $pO_2$  measurements were made in areas void of large feeding vessels and between capillaries. An average of 120 and 10  $pO_2$  measurements was made in each animal after the Random and Focused protocols, respectively.

### Comparison of tissue $pO_2$ histograms obtained from focused and random measurements

The present study was carried out to determine the distribution of tissue  $pO_2$  in the awake chamber-window model by using high-resolution phosphorescence quenching (13, 16, 21). Animals inspired either ambient air ( $FiO_2$ , 21%) or  $FiO_2$ , 100%, to investigate whether increasing intravascular  $pO_2$  would affect the homogeneity or the interstitial  $pO_2$  level or both. Measurements were performed in 11 animals, with five animals in each treatment group and one used for the study of the adjustable window size.

The  $pO_2$  distribution values obtained with the random and focused protocols during normoxia is presented in Fig. 2A and B, respectively. Figure 2C is the histogram obtained by using the random protocol during hyperoxia. The descriptive statistics of these data are summarized in Table 1.

The principal finding of this study is that tissue  $pO_2$  measured randomly by scanning the tissue along set paths without regard to microvascular structures has a gaussian distribution, average  $pO_2$  of  $25.1 \pm 8.9$  mm Hg ( $n = 550$ ,  $N = 5$  animals) and a maximum and minimum  $pO_2$  of 63.1 and 5.5 mm Hg, respectively.

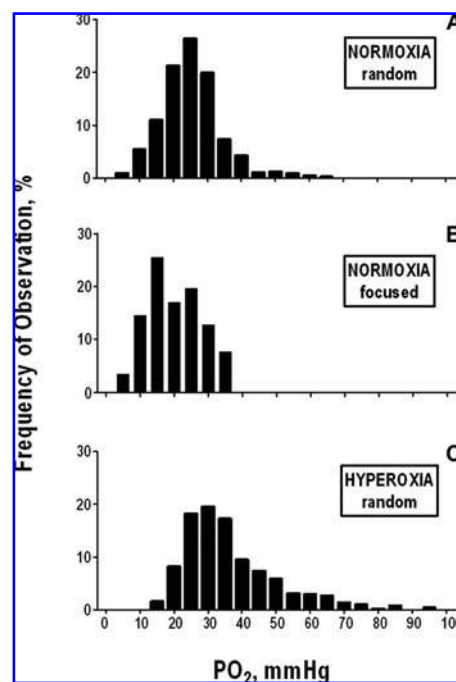


**FIG. 2. Interstitial  $pO_2$  levels in the hamster window-chamber model.** (A) Normoxia: random protocol ( $n = 536$ ;  $N = 5$ ). (B) Normoxia: focused protocol ( $n = 102$ ;  $N = 5$ ). (C), Hyperoxia: random protocol ( $n = 517$ ;  $N = 5$ ).

TABLE 1.

	<i>Normoxia (random)</i>	<i>Normoxia (focused)</i>	<i>Hyperoxia (random)</i>
N	5	5	5
mean $\pm$ std	25.1 $\pm$ 8.9	20.2 $\pm$ 7.7	36.8 $\pm$ 14.8
maximum	63.0	36.8	20.2
minimum	5.5	14.8	7.7
n	536	517	118

N, number of animals; mean, maximum, minimum pO<sub>2</sub> [=] mm Hg; n, number of measurements.

### Effect of the sensor size on tissue pO<sub>2</sub> histogram

The effect of doubling and quadrupling the 20  $\times$  20- $\mu$ m PQM window area on the pO<sub>2</sub> distribution is shown in Fig. 3. These data were obtained from a single animal in which the size of the window was sequentially changed at each measuring site, alternating from starting at 20  $\times$  20 or at 80  $\times$  80  $\mu$ m ( $n = 36$ ). No statistical significance was obtained between the pO<sub>2</sub> distributions constructed with the 20  $\times$  20 and 40  $\times$  40 windows, in which the mean and standard deviation was 26.2  $\pm$  5.6 and 25.0  $\pm$  6.1 mm Hg, respectively. When the window was increased to 80  $\times$  80  $\mu$ m, the distribution significantly shifted to lower pO<sub>2</sub> and had a lower standard deviation (19.6  $\pm$  4.7 mm Hg). These values were statistically significantly lower than those obtained with the smaller windows ( $p < 0.0001$ ). Tissue pO<sub>2</sub> by using the focused protocol was 21.7  $\pm$  3.5 mm Hg, which was not statistically different from

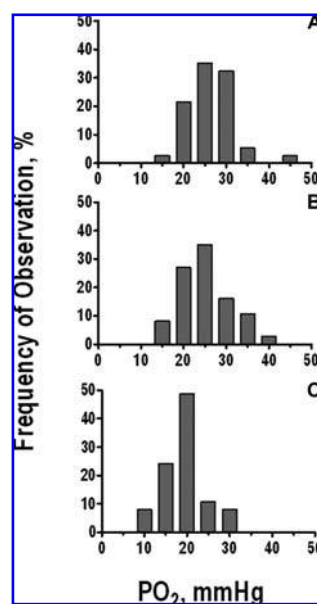


**FIG. 3.** The effect of the PQM window size on the interstitial pO<sub>2</sub> histograms. Measurements are made during normoxia in one animal ( $n = 36$ ). Histograms constructed from different window sizes (mean  $\pm$  SD, maximum, minimum). (A) 20  $\times$  20  $\mu$ m (26.2  $\pm$  5.6 mm Hg, 43.8, 12.7). (B) 40  $\times$  40  $\mu$ m (25.0  $\pm$  6.1 mm Hg, 37.6, 12.5). (C) 80  $\times$  80  $\mu$ m (19.6  $\pm$  4.7 mm Hg, 31.9, 10.5).

the results obtained with the 80  $\times$  80 window. Therefore, as the size of the window is increased, the average value of the distribution decreased. This result is a consequence of the nonlinear averaging of the long decay curves for the low levels, and the short decay for the higher pO<sub>2</sub> values, in which the phosphorescence signal is essentially zero during the period that the low-pO<sub>2</sub> signal remains significantly elevated. Thus, very few low-pO<sub>2</sub> values provide a larger contribution than many high-pO<sub>2</sub> values.

No statistical difference was found by using the smaller optical measuring windows in random locations. As expected, using the smaller measuring windows in selected focused locations provides the lowest tissue pO<sub>2</sub> determination, because it deliberately excludes measurements in the intravascular compartment, which always have higher values than the tissue, even in venules. The focused pO<sub>2</sub> value should closely correspond to the average value of the interstitial fluid pO<sub>2</sub>, where the phosphorescent marker is located. The finding that pO<sub>2</sub> determined with the larger 80  $\times$  80- $\mu$ m window is not statistically different from the most probable value of the interstitial pO<sub>2</sub> is interesting but probably fortuitous. Large windows are likely to contain a significant number of signals from the blood compartment, which complicates the averaging process because blood and tissue have different concentrations of the phosphorescent dye and different light absorptions characteristics. These considerations and findings illustrate the basic difficulty in interpreting tissue pO<sub>2</sub> measurements when it is not possible to obtain localized data at the microscopic level, in conditions in which the measurement location can be related to the microvascular anatomy.

### WHAT ARE THE UPPER LIMITS TO TISSUE pO<sub>2</sub> LEVELS?

Boeghold and Johnson (2) recorded, in 55- $\mu$ m-diameter arterioles of the cat sartorius muscle, a periaarteriolar pO<sub>2</sub> of 52.1  $\pm$  3.1 mm Hg (SEM) when tissue pO<sub>2</sub> was 22.8  $\pm$  3.3 mm Hg (SEM) by using Whalen microelectrodes. Using PQM, pO<sub>2</sub> values of 37  $\pm$  2 and 31  $\pm$  3 mm Hg were obtained in similar-sized arterioles and venules of the rat spinotrapezius muscle (15). Average tissue pO<sub>2</sub> was 19.3  $\pm$  1.6 mm Hg when mapped by using multiwire surface electrodes in the awake hamster window-chamber model (14). The pO<sub>2</sub> histograms constructed from these multiwire electrode maps did not show any values  $>40$  mm Hg. An extensive review of microvascular oxygen distributions (20) reports the highest pO<sub>2</sub> value recorded in 12 studies of arterioles  $\leq 100$   $\mu$ m, by using either the microelectrode or the phosphorescence technique, was  $\sim 80$  mm Hg, and the highest arterial pO<sub>2</sub> in the animals studied was 100 mm Hg. The highest pO<sub>2</sub> reported in eight studies of venules  $\leq 200$ - $\mu$ m diameter was  $\sim 40$  mm Hg.

Hamsters are fossorial animals and therefore are adapted to a low-oxygen and high-carbon dioxide atmosphere found in their natural habitat. Thus, hamsters have evolved to a low central arterial pO<sub>2</sub>. As an example, in the present study, mean arterial pO<sub>2</sub> measured from blood samples drawn from the catheter in the carotid artery was 60.5  $\pm$  5.2 mm Hg. It is therefore a legitimate concern whether the pO<sub>2</sub> distribution in the hamster window chamber is representative of similar tissues in other

species with normal arterial  $pO_2$  (skeletal muscle, adipose, and subcutaneous connective tissue). However, the  $pO_2$  in A0 arterioles of hamster is identical to that of other species (rats, mice, cats) not adapted to a fossorial environment). This is in part explained by the tissue of the chamber window in the hamster being supplied by a branch of the aorta, minimizing the lung/microcirculation  $pO_2$  longitudinal gradient. Thus, in principle, the  $pO_2$  distribution in the hamster microcirculation is the same as that of other species.

Further to validate this contention, we carried out the same study in conditions of hyperoxia, admittedly an extreme effect because this elevated arterial blood  $pO_2$  to  $478 \pm 20$  mm Hg. This extreme condition shifted the  $pO_2$  distribution to the right relative to normoxia ( $36.8 \pm 14.8$  mm Hg;  $n = 517$ ), as shown in Fig. 2A and C; however, it caused only a slight shift to the right of the tissue  $pO_2$  distribution. Notably, the high-end extremes of the hyperoxic  $pO_2$  random distribution were  $< 80$  mm Hg. Furthermore, the variability of the data increases, probably as a consequence of hyperoxia being vasoconstrictive, causing a significant decrease in functional capillary density (18).

### WHERE ARE THE LOWEST TISSUE $pO_2$ VALUES?

The lowest  $pO_2$  in the tissue recorded in the present study was 5.5 mm Hg during normoxic conditions. This value is within the range of those reported for the lymph in terminal lymphatics in the rat mesentery (11). In the present study, no attempt was made to correlate the underlying anatomy with the actual  $pO_2$  measurement. Our study provides no evidence for tissue  $pO_2$  being below  $\sim 5$  mm Hg. In a different study, histograms of intracellular recordings of muscle  $pO_2$  showed that the majority of cells were in the range of 0–5 mm Hg, with 38% being at  $\leq 1$  mm Hg (22). These results illustrate the presence of a tissue/mitochondria  $pO_2$  gradient; however, they are in contrast with results from studies using NADH fluorescence to determine anaerobic respiration in localized tissue areas in the exteriorized cat sartorius muscle (17). This study shows that only 3% of the tissue was on the verge of hypoxia ( $pO_2$ , 5–10 mm Hg), which was defined as the location where delay between blood-flow stoppage and the beginning of the increase of NADH fluorescence was  $\leq 10$  sec.

### COMPARISON AND INTERPRETATION OF TISSUE $pO_2$ HISTOGRAMS

Previous data in the literature obtained by using polarographic electrodes, mapping intravascular hemoglobin saturation, multiwire polarographic electrodes, and PQM concur with data obtained in the present study. Notably these results are qualitatively and quantitatively different from those obtained with a new technique for measuring different probes to assess intra- and extravascular  $pO_2$  (23). In this new technique, two different phosphorescence-quenching chromophores were delivered separately to the intravascularly and perivascular space in the thigh muscle of an awake mouse. Figure 4 compares the extravascular tissue  $pO_2$  distribution by using OXY-FLUOR G3 with that obtained by using the multiwire electrode mapping technique (14).

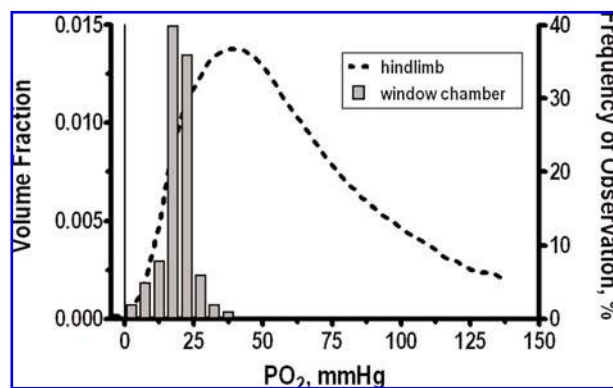


**FIG. 4. Interstitial  $pO_2$  distributions.** The plot is redrawn from the data from multiwire electrodes (14) and the new phosphorescence dyes by using the phosphorescence-quenching technique limited to the extravascular space (23). The multiwire electrode data are from the awake hamster window-chamber tissue (histogram, right y-axis) and is presented as the percentage frequency of observation. The data using the new Oxyphors are from awake murine hindlimb (line, left y-axis) and are presented as the fractional tissue volume interrogated by the sensor.

This recently reported dual phosphorescence quenching technique was developed to solve the possible detachment of the phosphorescence probe from its carrier protein, leading to extravasation of the dye, causing it to combine with proteins other than albumin. The detached dye could potentially react with other proteins, thus rendering the measurement of  $pO_2$  independent of light-excitation intensity, emission absorption, and dye concentration in the tissue. This problem does not appear to have significantly affected previous measurements of tissue  $pO_2$  made by using the palladium porphyrin bound to albumin *in vitro* and injected intravenously. This assertion is also validated by the direct study comparing tissue  $pO_2$  measurements by using the PQM and the polarographic electrode, which found no statistical difference between measurements (3).

PQM has been implemented in several laboratories, providing consistent intravascular  $pO_2$  data in the microcirculation. In general, no evidence exists for intravascular blood  $pO_2$  being  $< 20$  mm Hg at the microvascular level during normal conditions. The new technique shows that  $\geq 5\%$  of the measurements fall below this value. A curious result reported by Wilson *et al.* (23) is that  $\geq 20\%$  of blood  $pO_2$  measurements are  $> 100$  mm Hg, which is possible only if the preparation is exposed to 100% oxygen or there is a mechanism to concentrate oxygen as blood transits from the lungs to the site of measurement. The finding that 60% of the tissue has a  $pO_2 > 50$  mm Hg suggests that the method for reducing the oxygen-quenching signal into  $pO_2$  histograms distorts the data. It cannot be excluded that the direct injection of the porphyrin dye into the tissue without the protective association with albumin may induce production of significant quantities of oxygen free radicals, causing a severe metabolic impairment in the tissue. The effect of inhibiting tissue metabolism on the distribution of tissue  $pO_2$  was documented by an 80% exchange transfusion of molecular hemoglobin (4). Results showed that despite a reduced microvascular oxygen delivery



and extraction in the tissue of the hamster window chamber, the interstitial pO<sub>2</sub> was elevated above normal levels.

Our results show that the distribution of tissue pO<sub>2</sub>, when taken with the random protocol, which by chance would include measurements focused in blood vessels, yields a higher tissue pO<sub>2</sub>. Measurements deliberately made in areas void of vessels, thus avoiding intravascular measurements, yield a lower mean pO<sub>2</sub> value and standard deviation. The absolute value of the standard deviation is significant because it shows what percentage of the tissue may be anoxic. In the gaussian distribution, two standard deviations away from the mean represent 2.5% of the total tissue, a value similar to the 3.2% obtained in skeletal muscle pO<sub>2</sub> distribution by Toth *et al.* (17).

## CONCLUSIONS AND OPEN QUESTIONS

In summary, we show that in the tissue pO<sub>2</sub> of the hamster window chamber is fairly uniform, even in close proximity of arterioles and venules, because these present steep tissue gradients effectively isolate the tissue from the high arteriolar and venular pO<sub>2</sub>. In normal conditions, the pO<sub>2</sub> in the hamster window chamber is regulated at a level whereby none of the tissue is at risk of anoxia (<5 mm Hg). Hyperoxic inspiration did not change the tissue pO<sub>2</sub> distribution significantly, an effect that may be related to the intrinsic regulation of blood flow by intravascular pO<sub>2</sub> (18), and the increase in vessel-wall gradient and its oxygen consumption, which is a function of blood pO<sub>2</sub> (19). In conclusion, a precise and unambiguous use of the term tissue pO<sub>2</sub> requires the measurement of pO<sub>2</sub> at tissue locations sampled in areas of ~20- to 40- $\mu$ m diameter, mostly void of blood vessels. Finally, no evidence exists in this tissue for intra- or extravascular pO<sub>2</sub> >100 mm Hg, even during hyperoxia (18).

Thus, many questions still remain with regard to oxygen delivery to tissue. How is oxygen delivery managed to achieve a uniform interstitial level? During pathologic oxygen-delivery conditions, such as acute anemia (reduced oxygen-carrying capacity) and ischemia (low flow), how well does the tissue pO<sub>2</sub> predict adequate oxygen delivery to the mitochondria? Is the use of tissue pO<sub>2</sub> as a clinical marker to denote recovery of normal oxygenation conditions appropriate? Can it not also represent tissue that is metabolically impaired?

## APPENDIX

### Notes

#### 1. Animal Preparation

Investigations were performed in golden Syrian hamsters (Charles River Laboratories, Boston, MA). Animal handling and care were provided by following the procedures outlined in the Guide for the Care and Use of Laboratory Animals (1). The study was approved by the local Institutional Animal Care and Use Committee. The hamster window-chamber model is widely used for microvascular studies in unanesthetized conditions, and the complete surgical technique is described in detail elsewhere (5, 9). In brief, the animal was prepared for chamber implantation with a 50-mg/kg i.p. injection of pentobarbital sodium anesthesia. After hair removal, sutures were used to lift the dorsal skin away from the animal, and one frame of the chamber was positioned on the animal's back. A chamber consisted of two identical

titanium frames with a 15-mm circular window. With the aid of back-lighting and a stereomicroscope, one side of the skin fold was removed by following the outline of the window until only a thin layer of retractor muscle and the intact subcutaneous skin of the opposing side remained. Saline and then a coverglass were placed on the exposed skin, held in place by the other frame of the chamber. The intact skin of the other side was exposed to the ambient environment. The animal was allowed  $\geq 2$  days for recovery; afterward, its chamber was assessed under the microscope for any signs of edema, bleeding, or unusual neovascularization. Barring these complications, the animal was anesthetized again with pentobarbital sodium. Arterial and venous catheters (PE-50) were implanted in the carotid artery and jugular vein. The catheters were filled with a heparinized saline solution (30 IU/ml) to ensure their patency at the time of experiment. Catheters were tunneled under the skin and exteriorized at the dorsal side of the neck, where they were attached to the chamber frame with tape. Experiments were performed after  $\geq 24$  h and usually within 48 h after catheter implantation.

**Inclusion Criteria.** Animals were suitable for the experiments if their systemic parameters were within normal range: (a) heart rate (HR), >320 beats/min; (b) mean systemic blood pressure (MAP), >80 mm Hg; (c) systemic hematocrit (Hct), >45%; (d) systemic arterial pO<sub>2</sub>, >50 mm Hg. The microvasculature of the chamber tissue was examined under low (150x) and high (650x) magnification for edema and bleeding. Animals were excluded from the study if these signs of trauma were observed.

#### 2. Systemic parameters

MAP was tracked continuously over the entire experimental period and the HR determined from the pressure trace (Biopac, Santa Barbara, CA; Spectramed Pressure Transducer). Systemic hematocrit was measured from centrifuged arterial blood samples taken in heparinized capillary tubes (Readacrit Centrifuge, Clay Adams, Division of Becton and Dickinson, Parsippany, NJ). Arterial blood sampled from the carotid artery catheter into heparinized capillary tubes were immediately analyzed for pO<sub>2</sub> at 37°C (pH/blood gas analyzer, model 248, Bayer).

#### 3. Experimental protocol

The unanesthetized animal was placed in a restraining tube. A plastic tent with an inlet valve connected to a gas tank was placed in the front of the restraining tube. The gas flow rate (1.8 L/min) into the tent was diffused by a cotton-filter barrier so that the hamster was not subjected to a direct stream of gas flow. The restraining tube was attached to the stage of an intravital microscope (B $\times$ 51WI Olympus; Central Valley, PA) equipped with a water immersion 40x objective (Olympus Wplan; numerical aperture, 0.7). The tissue image was projected onto a CCD camera (COHU, San Diego 4815-2000) connected to a video cassette recorder and viewed on a monitor.

In this study, animals were divided into two treatment groups and were exposed to either FiO<sub>2</sub> 0.21 (Normoxic) or 1.0 (Hyperoxic); flow rate was 1.8 L/min. Baseline systemic parameters were assessed after the animal became accustomed with the tube and flow of FiO<sub>2</sub> of 0.21 ~15–20 min. The animals were then infused with the Pd-Phorphyrin dye, and the FiO<sub>2</sub> was switched to FiO<sub>2</sub> of 1.0 in the second group. The animal was given a 10-min rest for the dye to circulate and also for the animals in the hyperoxic group to reach a steady state and become accustomed to the increase in the oxygen content of the inspired air. Systemic parameters were then sampled again in the hyperoxic group to verify the increased arterial pO<sub>2</sub>. pO<sub>2</sub> measurements were then performed by following the Random and Focused Protocol. All measurements were completed within 45 min. One animal was used to study the effect of the size of the sensor window on the oxygen distribution. The size of the window was increased by two- and fourfold the normal 20  $\times$  20  $\mu$ m<sup>2</sup>.

#### 4. Data analysis

Results are presented as mean  $\pm$  SD unless otherwise noted. *N* denotes the number of animals within each treatment group, and *n* denotes the number of total measurements. The data were analyzed

by using *t* test and ANOVA with repeated measures, and when appropriate, Bonferroni multiple-comparison *post hoc* test was used to determine significance between groups. The nature of the distribution was quantified by using GraphPad Prism 4.01 (GraphPad Soft Ware, Inc., San Diego, CA).

## ACKNOWLEDGMENTS

This research was supported in part by the USPHS Bioengineering Research Partnership grant R24-HL 064395, grants R01-HL 062318, R01-HL 062354, and R01-HL 076182.

## ABBREVIATIONS

FiO<sub>2</sub>, fractional inspired oxygen; HCT, hematocrit; HR, heart rate; MAP, mean arterial pressure; *n*, number of measurements; *N*, number of animals; pO<sub>2</sub>, partial pressure of oxygen; PQM, phosphorescence-quenching microscopy.

## REFERENCES

1. National Research Council. *Guide for the care and use of laboratory animals*. Washington, DC: National Academy Press, 1996.
2. Boegehold MA and Johnson PC. Periarteriolar and tissue pO<sub>2</sub> during sympathetic escape in skeletal muscle. *Am J Physiol* 254: H929–H936, 1988.
3. Buerk DG, Tsai AG, Intaglietta M, and Johnson PC. *In vivo* hamster skin fold tissue pO<sub>2</sub> measurements by phosphorescence quenching and recessed pO<sub>2</sub> microelectrodes are in agreement. *Microcirculation* 5: 219–225, 1998.
4. Cabrales P, Tsai AG, and Intaglietta M. Deferoxamine lowers tissue damage after 80% exchange transfusion with polymerized hemoglobin. *Antioxid Redox Signal* 9: 375–384, 2007.
5. Colantuoni A, Bertuglia S, and Intaglietta M. Effects of anesthesia on the spontaneous activity of the microvasculature. *Int J Microcirc Clin Exp* 3: 13–28, 1984.
6. Duling BR and Berne RM. Longitudinal gradients in periarteriolar oxygen tension: a possible mechanism for the participation of oxygen in the local regulation of blood flow. *Circ Res* 27: 669–678, 1970.
7. Effros RM, Taki K, Reid E, and Silverman P. Countercurrent diffusion in the renal cortex of the rabbit. *Circ Res* 55: 463–467, 1984.
8. Ellsworth ML and Pittman RN. Arterioles supply oxygen to capillaries by diffusion as well as by convection. *Am J Physiol* 258: H1240–H1243, 1990.
9. Endrich B, Asaishi K, Götz A, and Messmer K. Technical report: a new chamber technique for microvascular studies in unanesthetized hamsters. *Res Exp Med* 177: 125–134, 1980.
10. Friesenecker B, Tsai AG, Dunser MW, Mayr AJ, Martini J, Knotzer H, Hasibeder W, and Intaglietta M. Oxygen distribution in microcirculation after arginine vasopressin-induced arteriolar vasoconstriction. *Am J Physiol Heart Circ Physiol* 287: H1792–H1800, 2004.
11. Hangai-Hoger N, Carales P, Briceno JC, Tsai AG, and Intaglietta M. Microlymphatic and tissue oxygen tension in the rat mesentery. *Am J Physiol Heart Circ Physiol* 286: H878–H883, 2004.
12. Kerger H, Groth G, Kalenka A, Vajkoczy P, Tsai AG, and Intaglietta M. pO<sub>2</sub> measurements by phosphorescence quenching: characteristics and applications of an automated system. *Microvasc Res* 65: 32–38, 2003.
13. Kerger H, Torres, Filho IP, Rivas M, Winslow RM, and Intaglietta M. Systemic and subcutaneous microvascular oxygen tension in conscious Syrian golden hamsters. *Am J Physiol* 267: H802–H810, 1995.
14. Nolte D, Steinhauser P, Pickelmann S, Berger S, Härtl R, and Messmer K. Effects of diaspirin-cross-linked hemoglobin (DCLHb) on local tissue oxygen tension in striated skin muscle: an efficacy study in the hamster. *J Lab Clin Med* 130: 328–338, 1997.
15. Smith LM, Barbee RW, Ward KR, and Pittman RN. Prolonged tissue pO<sub>2</sub> reduction after contraction in spinotrapezius muscle of spontaneously hypertensive rats. *Am J Physiol Heart Circ Physiol* 287: H401–H407, 2004.
16. Torres Filho IP, Kerger H, and Intaglietta M. pO<sub>2</sub> measurements in arteriolar networks. *Microvasc Res* 51: 202–212, 1996.
17. Toth A, Pal M, Tischler ME, and Johnson PC. Are there oxygen-deficient regions in resting skeletal muscle? *Am J Physiol* 270: H1933–H1939, 1996.
18. Tsai AG, Cabrales P, Winslow RM, and Intaglietta M. Microvascular oxygen distribution in awake hamster window chamber model during hyperoxia. *Am J Physiol Heart Circ Physiol* 285: H1537–H1545, 2003.
19. Tsai AG, Friesenecker B, Mazzoni MC, Kerger H, Buerk DG, Johnson PC, and Intaglietta M. Microvascular and tissue oxygen gradients in the rat mesentery. *Proc Natl Acad Sci U S A* 95: 6590–6595, 1998.
20. Tsai AG, Johnson PC, and Intaglietta M. Oxygen gradients in the microcirculation. *Physiol Rev* 83: 933–963, 2003.
21. Vanderkooi JM, Maniara G, Green TJ, and Wilson DF. An optical method for measurement of dioxygen concentration based upon quenching of phosphorescence. *J Biol Chem* 262: 5476–5482, 1987.
22. Whalen WJ and Nair P. Intracellular PO<sub>2</sub> and its regulation in resting skeletal muscle of the guinea pig. *Circ Res* 21: 251–261, 1967.
23. Wilson DF, Lee WM, Makonnen S, Finikova O, Apreleva S, and Vinogradov SA. Oxygen pressures in the interstitial space and their relationship to those in the blood plasma in resting skeletal muscle. *J Appl Physiol* 101: 1648–1656, 2006.

Address reprint requests to:

Amy G. Tsai

Department of Bioengineering, 0412

University of California, San Diego

La Jolla, CA 92093-0412

E-mail: agtsai@ucsd.edu

Date of first submission to ARS Central, February 27, 2007;  
date of acceptance, February 28, 2007.

**This article has been cited by:**

1. Todd V. Cartee, Kellie J. White, Marvin Newton-West, Robert A. Swerlick. 2011. Hypoxia and hypoxia mimetics inhibit TNF-dependent VCAM1 induction in the 5A32 endothelial cell line via a hypoxia inducible factor dependent mechanism. *Journal of Dermatological Science* . [[CrossRef](#)]
2. Helge Opdahl, Tævje A. Strømme, Lise Jørgensen, Livia Bajelan, Hans E. Heier. 2011. The acidosis-induced right shift of the HbO<sub>2</sub> dissociation curve is maintained during erythrocyte storage. *Scandinavian Journal of Clinical & Laboratory Investigation* **71**:4, 314-321. [[CrossRef](#)]
3. Amy G. Tsai , Pedro Cabrales , Marcos Intaglietta . 2010. The Physics of Oxygen Delivery: Facts and Controversies. *Antioxidants & Redox Signaling* **12**:6, 683-691. [[Abstract](#)] [[Full Text HTML](#)] [[Full Text PDF](#)] [[Full Text PDF with Links](#)]
4. Christina M. Lee, Damian C. Genetos, Alice Wong, Clare E. Yellowley. 2010. Prostaglandin expression profile in hypoxic osteoblastic cells. *Journal of Bone and Mineral Metabolism* **28**:1, 8-16. [[CrossRef](#)]
5. Nivaldo R. Villela, Pedro Cabrales, Amy G. Tsai, Marcos Intaglietta. 2009. MICROCIRCULATORY EFFECTS OF CHANGING BLOOD HEMOGLOBIN OXYGEN AFFINITY DURING HEMORRHAGIC SHOCK RESUSCITATION IN AN EXPERIMENTAL MODEL. *Shock* **31**:6, 646-653. [[CrossRef](#)]
6. Beatriz Y. Salazar Vázquez, Reto Wettstein, Pedro Cabrales, Amy G. Tsai, Marcos Intaglietta. 2008. Microvascular experimental evidence on the relative significance of restoring oxygen carrying capacity vs. blood viscosity in shock resuscitation. *Biochimica et Biophysica Acta (BBA) - Proteins and Proteomics* **1784**:10, 1421-1427. [[CrossRef](#)]
7. Jeremy P.T. Ward. 2008. Oxygen sensors in context. *Biochimica et Biophysica Acta (BBA) - Bioenergetics* **1777**:1, 1-14. [[CrossRef](#)]